# Depressing synapse as a detector of frequency change

Joanna Jędrzejewska-Szmek, Jaroslaw Żygierewicz


www.elsevier.com/locate/yjtbi

# Depressing synapse as a detector of frequency change

Joanna Jędrzejewska-Szmek, Jarosław Żygierewicz

PII: S0022-5193(10)00318-8
DOI: doi:10.1016/j.jtbi.2010.06.028
Reference: YJTBI 6048

To appear in: *Journal of Theoretical Biology*

Received date: 29 December 2009
Revised date: 9 April 2010
Accepted date: 19 June 2010

Cite this article as: Joanna Jędrzejewska-Szmek and Jarosław Żygierewicz, Depressing synapse as a detector of frequency change, *Journal of Theoretical Biology*, doi:10.1016/j.jtbi.2010.06.028

# Depressing synapse as a detector of frequency change[☆]

Joanna Jędrzejewska-Szmek[a,*], Jarosław Żygierewicz[a]

[a] *Department of Biomedical Physics, Institute of Experimental Physics, Warsaw University, ul. Hoża 69, 00-681 Warszawa, Poland. tel. (48 22) 5532126, fax (48 22) 6226154*

**Abstract**

In this article we discuss the short-term synaptic depression using a mathematical model. We derive the model of synaptic depression caused by the depletion of synaptic vesicles for the case of infinitely short stimulation time and show that the analytical formulas for the postsynaptic potential (PSP) and kinetic functions take simple closed form. A solution in this form allows an analysis of the characteristics of depression as a function of the models parameters and the derivation of analytic formulas for measures of short time synaptic depression commonly used in experimental studies. Those formulas are used to validate the model by fitting it to two types of synapses described in the literature. Given the fitted parameters we discuss the behavior of the synapse in situations involving frequency change. We also indicate a possible role of depressing synapses in information processing as not only a filter of high frequency input but as a detector of the return from high frequency stimulation to the stimulation within frequency band specific for a given synapse.

## 1. Introduction

Synaptic transmission across neocortical synapses is strongly activity dependent (Thomson, 1997). Short-term synaptic depression is commonly observed and not fully understood. There are many mechanisms that can contribute to it (Nadel et al., 1989; Destexhe et al., 1994a,b). The two that are most commonly discussed are depletion of synaptic vesicles and receptor desensitization.

In this article we focus on synaptic depression caused by the depletion of synaptic vesicles. This type of synaptic depression can be described by a model proposed by Tsodyks and Markram (1997) and is referred to as the TM-model. In the TM-model the synaptic connection is described as a system with three states of *resources* among which those resources flow with specific time constants. The total amount of resources is constant. These three states are: $E$ effective — the resources taking part in the synaptic transfer, $I$ inactive — resources that are not accessible, and $R$ recovered — resources that are ready to take part in the synaptic transfer. Each presynaptic action potential (AP) transfers a certain fraction—$U_{\mathrm{SE}}$ (utilization of synaptic efficacy)— of the recovered resources to the effective state, which first inactivates with the time constant $\tau_{\mathrm{i}}$ and then

[☆]This work was founded by grant N N518 380837 of Ministerstwo Nauki i Szkolnictwa Wyższego

[*]Corresponding author

*Email addresses:* asia@fuw.edu.pl (Joanna Jędrzejewska-Szmek), jarekz@fuw.edu.pl (Jarosław Żygierewicz)

recovers again with the time constant $\tau_{\mathrm{r}}$. The kinetic equations of the TM-model are:

$$\begin{aligned} \frac{dR}{dt} &= \frac{I}{\tau_{\mathrm{r}}} - U_{\mathrm{SE}} R\ \delta(t - t_{\mathrm{AP}}) \\ \frac{dE}{dt} &= -\frac{E}{\tau_{\mathrm{i}}} + U_{\mathrm{SE}} R\ \delta(t - t_{\mathrm{AP}}) \\ I &= 1 - R - E, \end{aligned} \tag{1}$$

The postsynaptic current (PSC) is proportional to the fraction of resources in the effective state, $E$:

$$I_{syn} = A_{\mathrm{SE}} R_{\mathrm{in}}\ E \tag{2}$$

where $A_{\mathrm{SE}}$ is the absolute synaptic efficacy—the maximum possible response in the case when all the resources are activated by a presynaptic AP, $R_{\mathrm{in}}$ denotes the input resistance of the postsynaptic membrane (resistance of the channels) and $\tau_{\mathrm{m}}$ is the membrane's time constant. The postsynaptic potential $V$ is given by:

$$\tau_{\mathrm{m}} \frac{dV}{dt} = -V + A_{\mathrm{SE}} R_{\mathrm{in}}\ E. \tag{3}$$

As was discussed in our previous paper (Mazurkiewicz et al., 2008) in order to fully specify the model mathematically the $\delta$ distribution in (1) has to be regularized. In that paper we used a step regularization of the delta function. The step's duration $\Delta t$ was generally considered to reflect the AP duration. Mazurkiewicz et al. (2008) found that the model's dependence on the duration of synaptic stimulation is minimal and it might be advisable to investigate the case when $\Delta t \to 0$. In the present paper we analyze the model behavior in that limit. This simplification gives better insight into the importance and influence of each parameter on the model's behavior.

## 2. Methods

### *2.1. Time evolution of the postsynaptic potential and the kinetic functions*

Let us consider a synapse modeled by (1) at time $t = t_{AP}$ was stimulated by an action potential. For time $t > t_{AP}$, if there are no further stimulations, the time evolution of the models variables $R$, $E$ and $V$ is given by:

$$\begin{aligned} R(t) &= 1 + \left( R_+ - \frac{E_+ \tau_{\mathrm{i}}}{\tau_{\mathrm{r}} - \tau_{\mathrm{i}}} - 1 \right) e^{-\frac{t - t_{\mathrm{AP}}}{\tau_{\mathrm{r}}}} + \frac{E_+ \tau_{\mathrm{i}}}{\tau_{\mathrm{r}} - \tau_{\mathrm{i}}} e^{-\frac{t - t_{\mathrm{AP}}}{\tau_{\mathrm{i}}}} \\ E(t) &= E_+ e^{-\frac{t - t_{\mathrm{AP}}}{\tau_{\mathrm{i}}}} \\ V(t) &= \frac{E_+ A_{\mathrm{SE}} R_{\mathrm{in}} \tau_{\mathrm{i}}}{\tau_{\mathrm{i}} - \tau_{\mathrm{m}}} \left( e^{-\frac{t - t_{\mathrm{AP}}}{\tau_{\mathrm{i}}}} - e^{-\frac{t - t_{\mathrm{AP}}}{\tau_{\mathrm{m}}}} \right) + V_+ e^{-\frac{t - t_{\mathrm{AP}}}{\tau_{\mathrm{m}}}} \end{aligned} \tag{4}$$

as the heterogeneous part of the equations, $U_{\mathrm{SE}} R\ \delta(t - t_{\mathrm{AP}})$, is omitted. The $R_-$, $E_-$, $V_-$ and $R_+$, $E_+$, $V_+$ are the values of $R(t)$, $E(t)$, $V(t)$ before the onset and after the offset of the action potential respectively.

In currently discussed limit of infinitely short stimulation time ($\Delta t \to 0$) the arrival of action potential caused the discontinuity in the state of model variables. The relations between the pre

and post stimulation $R(t)$, $E(t)$ and $V(t)$ can be found solving the equations (1) for finite duration of $\Delta t$ (cf Mazurkiewicz et al. (2008)) and taking the limit of $\Delta t \to 0$. In this way we obtained:

$$\begin{aligned} R_+ &= \lim_{\Delta t \to 0} R(t_0) = R_- \; e^{-U_{\mathrm{SE}}} \\ E_+ &= \lim_{\Delta t \to 0} E(t_0) = E_- + R_- \left(1 - e^{-U_{\mathrm{SE}}}\right) \\ V_+ &= \lim_{\Delta t \to 0} V(t_0) = V_- \end{aligned} \tag{5}$$

In all the following formulas, we are going to use notation:

$$u = 1 - e^{-U_{\mathrm{SE}}} \tag{6}$$

The convergence of finite $\Delta t$ solution to the limiting solution is illustrated in Fig. 1. If there is no stimulation of the synapse, the kinetic functions and the postsynaptic potential converge to the steady state conditions:

$$R_0 = 1, \quad E_0 = 0, \quad V_0 = 0 \tag{7}$$

The kinetic functions $E(t)$ and $R(t)$ and the post-synaptic potential $V(t)$ can also be easily found for a series of action potentials $i = 1, ..., n, n+1, ...$ arriving at times $t = \{t_{\mathrm{AP}_1}, ..., t_{\mathrm{AP}_n}, t_{\mathrm{AP}_{n+1}}\}$. For a period of $t \in \left(t_{\mathrm{AP}_n}, t_{\mathrm{AP}_{n+1}}\right)$, they are of the form:

$$\begin{aligned} R(t) &= 1 + \left(R_n - \frac{E_n \tau_{\mathrm{i}}}{\tau_{\mathrm{r}} - \tau_{\mathrm{i}}} - 1\right) e^{-\frac{t - t_{\mathrm{AP}_n}}{\tau_{\mathrm{r}}}} + \frac{E_n \tau_{\mathrm{i}}}{\tau_{\mathrm{r}} - \tau_{\mathrm{i}}} e^{-\frac{t - t_{\mathrm{AP}_n}}{\tau_{\mathrm{i}}}} \\ E(t) &= E_n e^{-\frac{t - t_{\mathrm{AP}_n}}{\tau_{\mathrm{i}}}} \\ V(t) &= \frac{E_n A_{\mathrm{SE}} R_{\mathrm{in}} \tau_{\mathrm{i}}}{\tau_{\mathrm{i}} - \tau_{\mathrm{m}}} \left(e^{-\frac{t - t_{\mathrm{AP}_n}}{\tau_{\mathrm{i}}}} - e^{-\frac{t - t_{\mathrm{AP}_n}}{\tau_{\mathrm{m}}}}\right) + V_n e^{-\frac{t - t_{\mathrm{AP}_n}}{\tau_{\mathrm{m}}}} \end{aligned} \tag{8}$$

The consecutive initial conditions can be found from a recursive formula:

$$\begin{aligned} R_{n+1} &= (1 - u) \left(1 + \left(R_n - \frac{E_n \tau_{\mathrm{i}}}{\tau_{\mathrm{r}} - \tau_{\mathrm{i}}} - 1\right) e^{-\frac{T}{\tau_{\mathrm{r}}}} + \frac{E_n \tau_{\mathrm{i}}}{\tau_{\mathrm{r}} - \tau_{\mathrm{i}}} e^{-\frac{T}{\tau_{\mathrm{i}}}}\right) \\ E_{n+1} &= E_n e^{-\frac{T}{\tau_{\mathrm{i}}}} \\ &\quad + u \left(1 + \left(R_n - \frac{E_n \tau_{\mathrm{i}}}{\tau_{\mathrm{r}} - \tau_{\mathrm{i}}} - 1\right) e^{-\frac{T}{\tau_{\mathrm{r}}}} + \frac{E_n \tau_{\mathrm{i}}}{\tau_{\mathrm{r}} - \tau_{\mathrm{i}}} e^{-\frac{T}{\tau_{\mathrm{i}}}}\right) \\ V_{n+1} &= V_n e^{-\frac{T}{\tau_{\mathrm{m}}}} \\ T &= t_{\mathrm{AP}_{n+1}} - t_{AP_n} \end{aligned} \tag{9}$$

*2.2. Measures of short-term synaptic depression*

Reports of experimental observations of the short term synaptic plasticity use a number of different characteristics of this phenomenon. There are at least three common inter-spike interval-dependent measures of the short-term synaptic depression: Paired Pulse Ratio (*PPR*) as in (Gompf and Allen, 2004), Paired Pulse Depression (*PPD*) as in (Bannister and Thomson, 2007) and II-PSP-Integral to I-PSP-Integral ratio as in (Thomson, 1997). One can also mention consecutive postsynaptic responses to dual presynaptic stimulation, e.g (Baldelli et al., 2007) (PSC) and (West et al., 2006)(PSP), or steady state PSC amplitude (Sun et al., 2005) .

In this study we concentrate on the first two Paired Pulse Ratio (*PPR*) and Paired Pulse Depression (*PPD*).

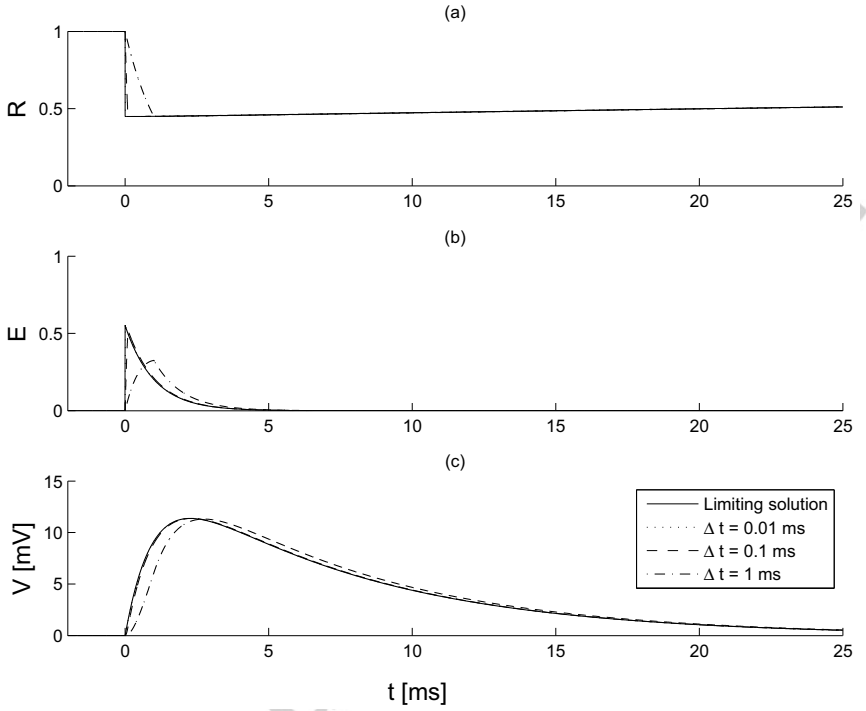


Figure 1: A comparison of the limiting solution and solutions of the kinetic functions and potential $V$ of the model with different stimulation duration $\Delta t$. The parameters used in computation are $\tau_{\mathrm{m}} = 7$ ms, $\tau_{\mathrm{i}} = 1$ ms, $\tau_{\mathrm{r}} = 200$ ms, $U_{\mathrm{SE}} = 0.8$, $A_{\mathrm{SE}} R_{\mathrm{in}} = 200$ mV, $\Delta t = \{\ 0.01$ ms, $\ 0.1$ ms, $\ 1$ ms$\}$. The biggest differences can be observed in the beginning of the build-up of PSP, but with decreasing $\Delta t$ they converge to the limiting solution (solid line).

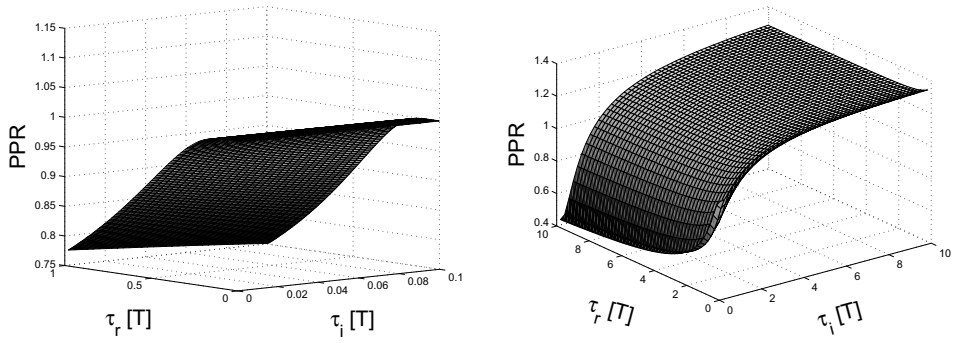


(a) (b)

Figure 2: Dependence of *PPR* on the time constants of the model: $\tau_{\mathrm{r}}$ and $\tau_{\mathrm{i}}$. The time constants once expressed in the units of interspike interval, $U_{\mathrm{SE}} = 0.95$. (a) The *PPR* for $\tau_{\mathrm{r}}$ and $\tau_{\mathrm{i}}$ in the physiological range for short time depression synapses. (b) The *PPR* for $\tau_{\mathrm{r}}$ and $\tau_{\mathrm{i}}$ of similar order, in the physiological range.

*2.2.1. Paired Pulse Ratio*

Following (Gompf and Allen, 2004; Dobrunz et al., 1997; Takayasu et al., 2006) we are going to define the Paired Pulse Ratio (*PPR*) as the ratio of the amplitude of the second postsynaptic current—$I_{syn_2}$ to the amplitude of the first one—$I_{syn_1}$. Substituting $E$ from (9) and (7) to (2) we obtain:

$$I_{syn_1} = uA_{\mathrm{SE}} \tag{10}$$

and:

$$I_{syn_2} = uA_{\mathrm{SE}}\left[1 + e^{-\frac{T}{\tau_{\mathrm{i}}}} + \frac{u}{\tau_{\mathrm{r}} - \tau_{\mathrm{i}}}\left(\tau_{\mathrm{i}} e^{-\frac{T}{\tau_{\mathrm{i}}}} - \tau_{\mathrm{r}} e^{-\frac{T}{\tau_{\mathrm{r}}}}\right)\right] \tag{11}$$

Using (10) and (11) one can derive the *PPR*:

$$PPR = \frac{I_{syn_2}}{I_{syn_1}} = 1 + e^{-\frac{T}{\tau_{\mathrm{i}}}} + u\frac{\tau_{\mathrm{i}} e^{-\frac{T}{\tau_{\mathrm{i}}}} - \tau_{\mathrm{r}} e^{-\frac{T}{\tau_{\mathrm{r}}}}}{\tau_{\mathrm{r}} - \tau_{\mathrm{i}}} \tag{12}$$

The interesting property of (12) is that it depends on the inter-spike interval $T$ only in the sense that $T$ scales the time. Please note that if the time is measured in the units of inter-spike interval the *PPR* reveals its dependence on the interplay between $\tau_{\mathrm{i}}$ and $\tau_{\mathrm{r}}$. The illustrative dependence of *PPR* on the time constants of the model - $\tau_{\mathrm{r}}$ and $\tau_{\mathrm{i}}$, measured in time units equal to $T$ and for typical $U_{SE} = 0.95$ is shown in Fig. 2. One can see that for parameters typical for a synapse displaying short term depression (Fig. 2(a)) there is a pronounced monotonic decrease of *PPR* with increasing $\tau_{\mathrm{r}}$. *PPR* also decreases with decreasing $\tau_{\mathrm{i}}$, however less dramatically than in case of the increasing $\tau_{\mathrm{r}}$. The lowest observed value of *PPR* of the synapse is 0.4.

This behavior is similar in case of smaller $U_{\mathrm{SE}}$ values.

In case of $\tau_{\mathrm{r}}$ and $\tau_{\mathrm{i}}$ larger than $T$ one can see PSC summation (Fig. 2(b)), as anticipated by Destexhe et al. (1994a,b).

*2.2.2. Paired Pulse Depression*

Paired Pulse Depression is a common measure of short-term synaptic depression, e.g. (Bannister and Thomson, 2007). It is defined as the inter-spike interval-dependent ratio of the amplitude of the second PSP to the first PSP.

The amplitude of the first PSP can be derived from (9) and (7):

$$V_1 = \frac{uA_{\mathrm{SE}}R_{\mathrm{in}}\tau_{\mathrm{i}}}{\tau_{\mathrm{i}}-\tau_{\mathrm{m}}}\left(\left(\frac{\tau_{\mathrm{i}}}{\tau_{\mathrm{m}}}\right)^{\frac{-\tau_{\mathrm{m}}}{\tau_{\mathrm{i}}-\tau_{\mathrm{m}}}} - \left(\frac{\tau_{\mathrm{i}}}{\tau_{\mathrm{m}}}\right)^{\frac{-\tau_{\mathrm{i}}}{\tau_{\mathrm{i}}-\tau_{\mathrm{m}}}}\right) \tag{13}$$

The amplitude of the second PSP is given by:

$$V_2 = \frac{A_{\mathrm{SE}}R_{\mathrm{in}}\tau_{\mathrm{i}}e_2}{\tau_{\mathrm{i}}-\tau_{\mathrm{m}}}x^{-\frac{\tau_{\mathrm{m}}}{\tau_{\mathrm{i}}-\tau_{\mathrm{m}}}} + \left(v_2 - \frac{A_{\mathrm{SE}}R_{\mathrm{in}}\tau_{\mathrm{i}}e_2}{\tau_{\mathrm{i}}-\tau_{\mathrm{m}}}\right)x^{-\frac{\tau_{\mathrm{i}}}{\tau_{\mathrm{i}}-\tau_{\mathrm{m}}}} \tag{14}$$

Constants $e_2$ and $v_2$ can be found using (9):

$$\begin{aligned} e_2 &= u\left[1 + e^{-\frac{T}{\tau_{\mathrm{i}}}} + \frac{u}{\tau_{\mathrm{r}}-\tau_{\mathrm{i}}}\left(\tau_{\mathrm{i}}e^{-\frac{T}{\tau_{\mathrm{i}}}} - \tau_{\mathrm{r}}e^{-\frac{T}{\tau_{\mathrm{r}}}}\right)\right] \\ v_2 &= \frac{uA_{\mathrm{SE}}R_{\mathrm{in}}\tau_{\mathrm{i}}}{\tau_{\mathrm{i}}-\tau_{\mathrm{m}}}\left(e^{-\frac{T}{\tau_{\mathrm{i}}}} - e^{-\frac{T}{\tau_{\mathrm{m}}}}\right) \end{aligned} \tag{15}$$

Using (13), (14) and (12) one can find the formula describing *PPD*:

$$\begin{aligned} PPD &= \frac{PPR\, x^{\frac{\tau_{\mathrm{m}}}{\tau_{\mathrm{m}}-\tau_{\mathrm{i}}}} + (v_1 - PPR)\, x^{\frac{\tau_{\mathrm{i}}}{\tau_{\mathrm{m}}-\tau_{\mathrm{i}}}}}{\left(\frac{\tau_{\mathrm{i}}}{\tau_{\mathrm{m}}}\right)^{\frac{\tau_{\mathrm{m}}}{\tau_{\mathrm{m}}-\tau_{\mathrm{i}}}} - \left(\frac{\tau_{\mathrm{i}}}{\tau_{\mathrm{m}}}\right)^{\frac{\tau_{\mathrm{i}}}{\tau_{\mathrm{m}}-\tau_{\mathrm{i}}}}} \\ x &= \frac{\tau_{\mathrm{i}}}{\tau_{\mathrm{m}}}\left(1 - \frac{v_1}{PPR}\right) \\ v_1 &= e^{-\frac{T}{\tau_{\mathrm{i}}}} - e^{-\frac{T}{\tau_{\mathrm{m}}}} \end{aligned} \tag{16}$$

In case of a wider inter-spike interval and smaller values of $\tau_{\mathrm{m}}$ *PPD* can be approximated by following formula:

$$PPD \approx PPR + \frac{v_1}{\left(\frac{\tau_{\mathrm{i}}}{\tau_{\mathrm{m}}}\right)^{\frac{\tau_{\mathrm{i}}}{\tau_{\mathrm{m}}}} - 1} \tag{17}$$

*2.3. Measures of synapse response to a change in incoming spikes frequency*

One of the possible ways of neural signaling is rate-coding. In this case is expressed by changing the frequency of the spikes arriving to the synapse. An interesting issue is how the information is processed at the depressing synapse.

Let us assume that the synapse was stimulated with frequency $f$ for time long enough to reach an asymptotic steady state values of variables $R$ and $E$:

$$\begin{aligned} R_{\mathrm{st}} &= \frac{(1-u)\left(1-e^{-\frac{1}{f\,\tau_{\mathrm{r}}}}\right)\left(1-e^{-\frac{1}{f\,\tau_{\mathrm{i}}}}\right)}{\left(1-(1-u)\,e^{-\frac{1}{f\,\tau_{\mathrm{r}}}}\right)\left(1-e^{-\frac{1}{f\,\tau_{\mathrm{i}}}}\right) - u\left(e^{-\frac{1}{f\,\tau_{\mathrm{r}}}} - e^{-\frac{1}{f\,\tau_{\mathrm{i}}}}\right)^{\frac{\tau_{\mathrm{i}}}{\tau_{\mathrm{i}}-\tau_{\mathrm{r}}}}} \\ E_{\mathrm{st}} &= \frac{u\left(1-e^{-\frac{1}{f\,\tau_{\mathrm{r}}}}\right)}{\left(1-(1-u)\,e^{-\frac{1}{f\,\tau_{\mathrm{r}}}}\right)\left(1-e^{-\frac{1}{f\,\tau_{\mathrm{i}}}}\right) - u\left(e^{-\frac{1}{f\,\tau_{\mathrm{r}}}} - e^{-\frac{1}{f\,\tau_{\mathrm{i}}}}\right)^{\frac{\tau_{\mathrm{i}}}{\tau_{\mathrm{i}}-\tau_{\mathrm{r}}}}} \end{aligned} \tag{18}$$

Next, let us assume that at certain moment the frequency of incoming spikes changes from $f$ to $F$. This means that the interval between the spikes changes to $1/F$. The amplitudes of the kinetic functions $R$ and $E$ after this interval are:

$$\begin{aligned} R_{\mathrm{I}} &= (1-u)\left(1+\left(R_{\mathrm{st}}-\frac{E_{\mathrm{st}}\tau_{\mathrm{i}}}{\tau_{\mathrm{r}}-\tau_{\mathrm{i}}}-1\right)e^{-\frac{1}{F\tau_{\mathrm{r}}}}+\frac{E_{\mathrm{st}}\tau_{\mathrm{i}}}{\tau_{\mathrm{r}}-\tau_{\mathrm{i}}}e^{-\frac{1}{F\tau_{\mathrm{i}}}}\right) \\ E_{\mathrm{I}} &= E_{\mathrm{st}}e^{-\frac{1}{F\tau_{\mathrm{i}}}}+u\left(1+\left(R_{\mathrm{st}}-\frac{E_{\mathrm{st}}\tau_{\mathrm{i}}}{\tau_{\mathrm{r}}-\tau_{\mathrm{i}}}-1\right)e^{-\frac{1}{F\tau_{\mathrm{r}}}}+\frac{E_{\mathrm{st}}\tau_{\mathrm{i}}}{\tau_{\mathrm{r}}-\tau_{\mathrm{i}}}e^{-\frac{1}{F\tau_{\mathrm{i}}}}\right) \end{aligned} \tag{19}$$

After the second interval of duration $1/F$ the amplitudes are:

$$\begin{aligned} R_{\mathrm{II}} &= (1-u)\left(1+\left(R_{\mathrm{I}}-\frac{E_{\mathrm{I}}\tau_{\mathrm{i}}}{\tau_{\mathrm{r}}-\tau_{\mathrm{i}}}-1\right)e^{-\frac{1}{F\tau_{\mathrm{r}}}}+\frac{E_{\mathrm{I}}\tau_{\mathrm{i}}}{\tau_{\mathrm{r}}-\tau_{\mathrm{i}}}\right) \\ E_{\mathrm{II}} &= E_{\mathrm{I}}e^{-\frac{1}{F\tau_{\mathrm{i}}}}+u\left(1+\left(R_{\mathrm{I}}-\frac{E_{\mathrm{I}}\tau_{\mathrm{i}}}{\tau_{\mathrm{r}}-\tau_{\mathrm{i}}}-1\right)e^{-\frac{1}{F\tau_{\mathrm{r}}}}+\frac{E_{\mathrm{I}}\tau_{\mathrm{i}}}{\tau_{\mathrm{r}}-\tau_{\mathrm{i}}}e^{-\frac{1}{F\tau_{\mathrm{i}}}}\right) \end{aligned} \tag{20}$$

There are two interesting ratios characterizing the reaction of the synapse to the change of the frequency of incoming spikes — one of $E_{\mathrm{I}}$ (19) to $E_{st}$ (18), let us name it $A_{\mathrm{I}}$,

$$A_{\mathrm{I}} = \frac{E_{\mathrm{I}}}{E_{\mathrm{st}}} \tag{21}$$

and the other of $E_{\mathrm{II}}$ (20) to $E_{\mathrm{I}}$ (19), let us name it $A_{\mathrm{II}}$:

$$A_{\mathrm{II}} = \frac{E_{\mathrm{II}}}{E_{\mathrm{I}}}. \tag{22}$$

In the case of $\tau_{\mathrm{r}} \gg \tau_{\mathrm{i}}$ one can omit the terms dependent on $\tau_{\mathrm{i}}$ (or take them to the appropriate limit). $A_{\mathrm{I}}$ is of the form:

$$A_{\mathrm{I}} = 1-u+\frac{u\left(1-e^{-\frac{1}{F\tau_{\mathrm{r}}}}\right)}{1-e^{-\frac{1}{f\tau_{\mathrm{r}}}}} \tag{23}$$

As one can see, its dependence on $F$ is exponential. For frequencies $f$ and parameters in the physiological region it is linear, so in the case of $\tau_{\mathrm{r}} f \ll 1$ for constant $F$, this formula takes linear form:

$$A_{\mathrm{I}} = 1-u+f\tau_{\mathrm{r}}u\left(1-e^{-\frac{1}{\tau_{\mathrm{r}}F}}\right) \tag{24}$$

$A_{\mathrm{II}}$ is given by:

$$A_{\mathrm{II}} = 1+(1-u)e^{-\frac{1}{F\tau_{\mathrm{r}}}}\left(1-\frac{1-e^{-\frac{1}{f\tau_{\mathrm{r}}}}}{1-(1-u)e^{-\frac{1}{f\tau_{\mathrm{r}}}}-ue^{-\frac{1}{F\tau_{\mathrm{r}}}}}\right) \tag{25}$$

$A_{\mathrm{II}}$ reaches maximum for:

$$F_{\max} = -\left(\tau_{\mathrm{r}}\log u^{-1}\left(\left(1-(1-u)e^{-\frac{1}{f\tau_{\mathrm{r}}}}\right)+\sqrt{\left(1-(1-u)e^{-\frac{1}{f\tau_{\mathrm{r}}}}\right)\left(1-e^{-\frac{1}{f\tau_{\mathrm{r}}}}\right)}\right)\right)^{-1} \tag{26}$$

| parameter | value | 68% confidence in | range and source |
|---|---|---|---|
| $\tau_{\mathrm{r}}$ | 282 ms | $(256, 308)$ ms | $(30, 1000)$ ms (Stevens and Wang, 1995) |
| $\tau_{\mathrm{i}}$ | 1 ms | $(1, 9)$ ms | $(1, 20)$ ms (Wall, 2005) |
| $U_{\mathrm{SE}}$ | 0.91 | (0.86,0.95) | (0.15,0.95) (Tsodyks and Markram, 1997) |

Table 1: The values of parameters estimated by fitting of *PPR* (12) to experimental data from (Gompf and Allen, 2004). The rightmost column displays plausible ranges of a given parameter reported in the indicated literature sources.

## 3. Results

### *3.1. Verification of the model: a fit to the experimental data*

To verify the model we fitted it to data measured for eight different types of synapses described respectively by Gompf and Allen (2004) and Petersen (2002) and Bannister and Thomson (2007).

The current model has the following parameters $Par = \{A_{\mathrm{SE}}R_{\mathrm{in}}, \tau_{\mathrm{m}}, \tau_{\mathrm{r}}, \tau_{\mathrm{i}}, U_{\mathrm{SE}}\}$. Some of them can be fixed to values known from direct measurements and the parameters $A_{\mathrm{SE}}R_m$ and $\tau_{\mathrm{m}}$ can be adjusted so that the PSP amplitude, rise-time, and the width of the half-amplitude agree with those measured experimentally or calculated using the membrane conductance and resistance values. The remaining parameters $\tau_{\mathrm{i}}$ and $U_{\mathrm{SE}}$ are difficult to measure directly. We estimated them by fitting the formula (12) in case of data reported in Gompf and Allen (2004) and formula (16) and normalized amplitude of the 10th PSP for data reported in Petersen (2002). In case of six datasets from Gompf and Allen (2004) we fitted (16) and 10%-90% PSP rise-time and PSP width of the half-amplitude (the two latter were computed by numerically solving the equation (28)). As the fitting procedure we utilized the scan of the parameter space in search for the minimum of the weighted sum of squared residua.

#### *3.1.1. Fit to the dataset I: the synapses of hypothalamic suprachiasmatic nuclei of juvenile rats*

The mammalian SCN are the site of an endogenous, self-sustained circadian timekeeper that provides temporal information for a wide range of physiological processes and behaviors. The circadian rise and fall of excitability of SCN neurons results in a circadian rhythm of peak ensemble action potential firing frequency which occurs during the middle of the day (Inouye and Kawamura, 1979). The synapses reported by Gompf and Allen (2004) came from juvenile rat hypothalamic suprachiasmatic nuclei (SCN). The analyzed synapses were GABAergic and they were extracted during the light phase. The observed depression phenomenon seemed to originate from the depletion of synaptic vesicles (Gompf and Allen, 2004).

We used formula (12) to estimate the parameters $\tau_{\mathrm{r}}$, $\tau_{\mathrm{i}}$ and $U_{\mathrm{SE}}$, since the data were obtained in a paired pulse experiment. The parameters of the current model were fitted to the data presented in Fig. 1(e) of Gompf and Allen (2004). The estimated parameters and confidence interval are presented in Tab. 1 together with plausible ranges of the parameters found in the literature. The fitted curve is shown in Fig. 3. It represents a reasonable fit to the experimental data ($\chi^2 = 0.7$ per degree of freedom) and the estimated parameters are in the physiologically plausible range.

#### *3.1.2. Fit to the dataset II: Excitatory connections of rat's layer 4 barrel cortex.*

As the second dataset for validation of the current model we utilized the data concerning synapses from layer 4 of somatosensory barrel cortex of juvenile rat reported by Petersen (2002), shown in Fig. 3(B) and 5(C). The data in Fig. 3(B) presents dependence of the *PPD* on inter-spike interval and the data in Fig. 5(C) presents the dependence of amplitudes ratio of $10^{th}$ EPSP to the

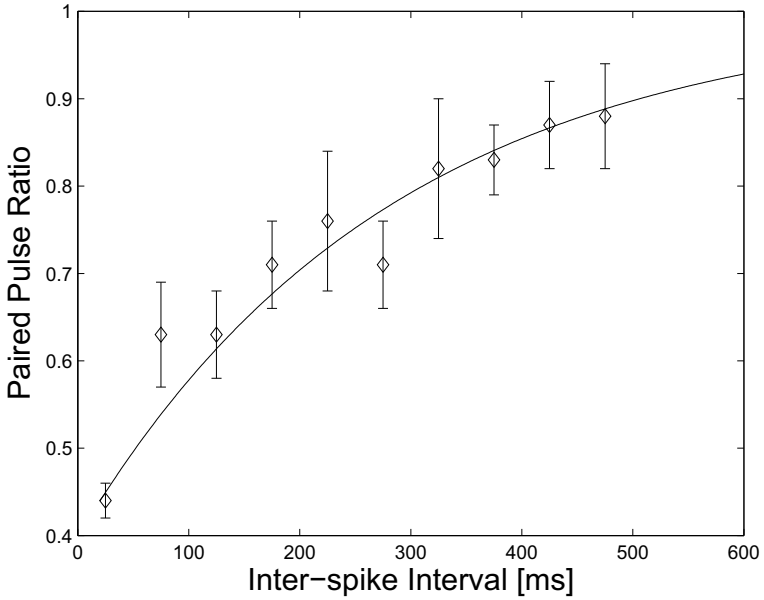


Figure 3: The experimental data from Fig. 1(e) of Gompf and Allen (2004) and the fitted curve (12). The parameters of the fitted model and their confidence intervals are presented in Tab. 1.

| parameter | value | 68% confidence in | range and source |
|---|---|---|---|
| $\tau_{\mathrm{r}}$ | 500 ms | $(467, 533)$ ms | $(30, 1000)$ ms (Stevens and Wang, 1995)<br>$(370, 580)$ ms (Petersen, 2002) |
| $\tau_{\mathrm{i}}$ | 1 ms | $(1, 2)$ ms | $(1, 20)$ ms (Wall, 2005) |
| $U_{\mathrm{SE}}$ | 0.61 | (0.57,0.65) | (0.15,0.95) (Tsodyks and Markram, 1997) |
| $\tau_{\mathrm{m}}$ | 1 ms | $(0.9, 1.1)$ ms | $(1, 100)$ ms |

Table 2: The values of parameters estimated by fitting of *PPD* (16) and the ratio of $10^{th}$ to the $1^{st}$ EPSP amplitude to experimental data from (Petersen, 2002). The rightmost column displays plausible ranges of a given parameter reported in the indicated literature sources.

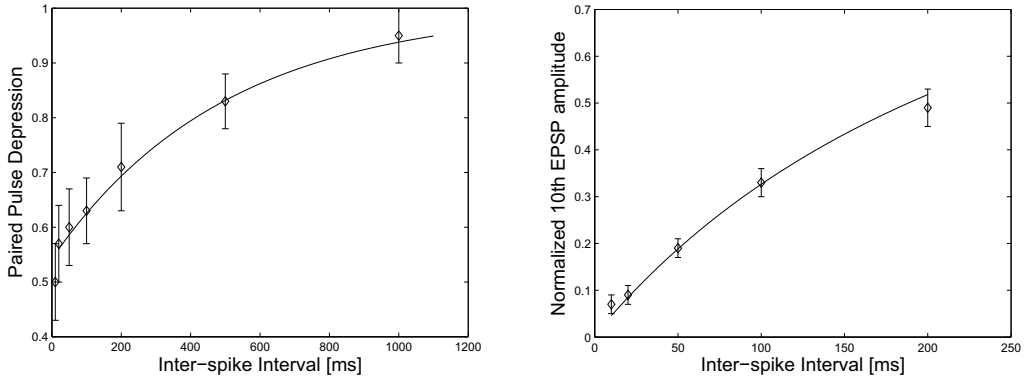


(a) (b)

Figure 4: The experimental data in Petersen (2002) and the fitted curve. (a) The *PPD* values from (Petersen, 2002) and the best-fit curve. (b) The normalized 10th EPSP amplitudes from (Petersen, 2002) and the best-fit curve. The parameters of the fit, their confidence intervals and ranges can be found in Tab. 2.

$1^{st}$ EPSP on inter-spike interval. Taken together the data constitute a unique set of two measures of depression obtained from the same synapses. A reasonable model should represent both types of dependencies with a single set of parameters.

We performed a simultaneous fit of the model to the data of both depression measures. The fit was performed by scanning the parameter space in search of the minimum of the weighted sum of the squared residua. For data taken from Fig. 3(B) the fitted function was *PPD* (16) and for the points in Fig. 5(C) the ratio of amplitude of $10^{th}$ EPSP to the amplitude of the $1^{st}$ EPSP[1]. Both types of experimental points — the *PPD* and the normalized $10^{th}$ EPSP amplitudes had equal weights in the fit. For the values of parameters reported in Tab. 2 we obtained a reasonable fit with $\chi^2 = 0.75$. The fit of *PPD* (16) curve is shown in Fig. 4(a) and the fit of the normalized $10^{th}$ PSP amplitude is displayed in Fig. 4(b). The obtained recovery constant $\tau_{\mathrm{r}}$ is concordant with the one obtained in (Petersen, 2002) and recovery constants obtained for other pyramidal neurons, e.g. (Varela et al., 1997, 1999; Finnerty et al., 1999; Markram et al., 1998).

[1]The amplitude of $10^{th}$ EPSP were calculated iteratively using (8).

*3.1.3. Connections made by pyramid neurons of adult male rats and cats from Bannister and Thomson (2007)*

We present here the fit to the data shown in Fig. 3 of (Bannister and Thomson, 2007). This experimental data was obtained in the paired pulse depression (*PPD*) experiment. The data was derived for three types of synapses from adult rats and cats. The types of measured synapses were:

- pyramid-pyramid connections in layer 4 further denoted as L4-L4
- pyramid-pyramid connections in layer 3 further denoted as L3-L3
- layer 4 spiny cells to layer 3 pyramid pairs further denoted as L4-L3

The points in Fig. 3 of (Bannister and Thomson, 2007) show the ratios of the amplitude of 2nd PSP decreased by the amplitude of the 1st PSP in time of the inter-spike interval. Hence, we fitted the following formula to the experimental data:

$$\begin{aligned} PPD_{\text{shifted}}(T) &= PPD(T) - \frac{e^{-\frac{T}{\tau_{\text{m}}}} - e^{-\frac{T}{\tau_{\text{i}}}}}{e^{-\frac{T_{\max}}{\tau_{\text{m}}}} - e^{-\frac{T_{\max}}{\tau_{\text{i}}}}} \\ T_{\max} &= \frac{\tau_{\text{i}}\tau_{\text{m}}}{\tau_{\text{i}} - \tau_{\text{m}}} \log \frac{\tau_{\text{i}}}{\tau_{\text{m}}} \end{aligned} \tag{27}$$

As one can see in Fig. 3 of (Bannister and Thomson, 2007) there are only six experimental points per dataset, and the model fitted to the data has four free parameters. In order to increase number of constraints we also included the data of 10%-90% EPSP rise-time and the EPSP width of the half-amplitude in the fitting procedure. The two latter constraints were included by solving following equation:

$$e^{-\frac{t}{\tau_{\text{i}}}} - e^{-\frac{t}{\tau_{\text{m}}}} - a\left(e^{-\frac{T_{\max}}{\tau_{\text{i}}}} - e^{-\frac{T_{\max}}{\tau_{\text{m}}}}\right) = 0, \tag{28}$$

where $a$ is the corresponding fraction of the EPSP amplitude.

The set of experimental points depends only on four of the model's parameters: $\tau_{\text{i}}$,$\tau_{\text{r}}$, $\tau_{\text{m}}$ and $U_{\text{SE}}$. The four parameters $\tau_{\text{r}}$, $\tau_{\text{i}}$, $U_{\text{SE}}$ and $\tau_{\text{m}}$ were scanned in their physiological regions as in Tab. 4.

The best-fit parameters minimize the sum of the squared residuals. The uncertainty of determined parameters was calculated using the standard method, the second derivative of the sum of squared residuals.

The best-fit curve and experimental data can be found in Fig. 5(a), 5(b) and 5(c). The *PPD* (27) seems to be a good fit to the experimental data, the calculated $\chi^2$ per degree of freedom was in range (0.5 1). The uncertainty of the fitted model partameters is high due to the uncertainty of the experimental data. O

Comparing the obtained recovery constants obtained fitting the three-step model and the two-step model (single-exponential decay constant) shown in Tab. 3 one can observe that in case of shorter $\tau_{\text{r}}$ the intrinsic dynamics of the recovery and effective fraction might be important. Even though the inactivation time-constant is an order of amplitude smaller than the recovery constant using the three-step model might provide more accuracy in simulations and in analysis.

*3.2. Reaction of the model synapse to the change in the inter-spike interval of incoming action potentials*

In section 2.3 we introduced two measures $A_{\text{I}}$ (21) and $A_{\text{II}}$ (22) of synaptic response to a change in incoming spikes frequency. In this subsection we use those measures to analyze the behavior of

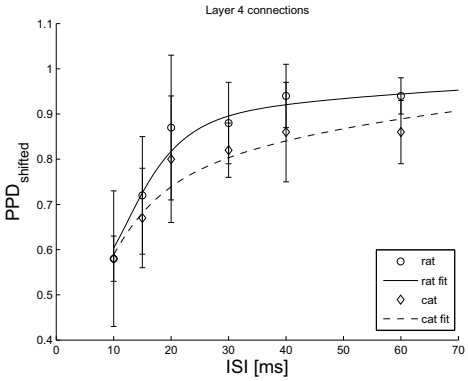


(a) Layer 4 pyramid-pyramid pairs

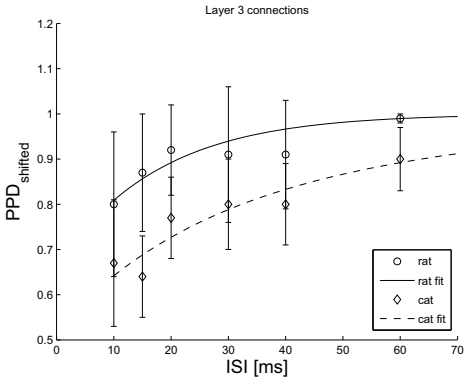


(b) Layer 3 pyramid-pyramid pairs

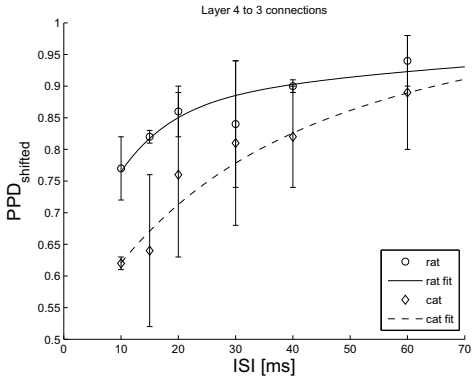


(c) Layer 4 spiny cells to layer 3 pyramid pairs

Figure 5: The experimental data in (Bannister and Thomson, 2007) and the fitted curve. The parameters of the fit and their confidence intervals can be found in Tab. 3, the parameters ranges and sources in Tab. 4.

the eight types of synapses (reported in (Gompf and Allen, 2004), (Petersen, 2002) and in (Bannister and Thomson, 2007)) that the model was fitted to in the previous subsection.

Figures 6, 7 and 8 show the measures $A_{\mathrm{I}}(f, F)$ and $A_{\mathrm{II}}(f, F)$ as functions of two frequencies. One, $f$, is the frequency spikes arrival to the synapse for time long enough to reach the stationary amplitudes of postsynaptic currents and the other is the new frequency, $F$. The frequency range of the stationary mode and the novel frequency was chosen according to the physiological properties of the presynaptic neurons, thus for the rat SCN it was set to $0 - 60\,\mathrm{Hz}$ and for synapses from layer 4 of somatosensory barrel cortex and in layer 4, layer 3 and layer 4 to layer 3 connections in rat and cat, it was set to $0 - 100\,\mathrm{Hz}$.

For the synapses with $\tau_{\mathrm{r}} \gg \tau_{\mathrm{i}}$ the ratio $A_{\mathrm{I}}(f, F)$ has similar behavior (Fig. 6(a), 6(c), 7(a), 7(e), 8(a)-8(e)). It reaches high values in case of a change from high frequency $f$ to low frequency $F$. These values monotonically decrease with the decrease of the difference between $f$ and $F$. This behavior is easy to understand. It means that after a long time of stimulation the recovered

| Type of connection | $\tau_{\mathrm{r}}$ | single-exponential decay (Bannister and Thomson, 2007) | $U_{\mathrm{SE}}$ | $\tau_{\mathrm{i}}$ | $\tau_{\mathrm{m}}$ |
|---|---|---|---|---|---|
| rat L4-L4 | $61 \pm 3$ ms | 17 ms | $0.15 \pm 0.06$ | $4 \pm 2$ ms | $5 \pm 2.5$ ms |
| cat L4-L4 | $57 \pm 12$ ms | 8 ms | $0.37 \pm 0.05$ | $1.5 \pm 0.4$ ms | $7 \pm 2$ ms |
| rat L4-L3 | $99 \pm 9$ ms | 4.4 ms | $0.15 \pm 0.01$ | $1 \pm 0.2$ ms | $8.5 \pm 0.2$ ms |
| cat L4-L3 | $47 \pm 3$ ms | 21 ms | $0.34 \pm 0.01$ | $12.5 \pm 0.3$ ms | $1 \pm 0.1$ ms |
| rat L3-L3 | $18 \pm 12$ ms | 12 ms | $0.15 \pm 0.11$ | $1 \pm 0.8$ ms | $16 \pm 1$ ms |
| cat L3-L3 | $54 \pm 10$ ms | 22 ms | $0.36 \pm 0.07$ | $1 \pm 0.8$ ms | $17.5 \pm 8$ ms |

Table 3: The best-fit parameters of the fit of $PPD_{\mathrm{shifted}}$ (27) to the experimental data in (Bannister and Thomson, 2007).

| parameter | range |
|---|---|
| $\tau_{\mathrm{r}}$ | $(4, 1000)$ ms from (Bannister and Thomson, 2007) |
| $U_{\mathrm{SE}}$ | (0.15,0.95) from (Tsodyks and Markram, 1997) |
| $\tau_{\mathrm{i}}$ | $(1, 20)$ ms from i.e. (Wall, 2005) |
| $\tau_{\mathrm{m}}$ | $(1, 100)$ ms |

Table 4: The range of parameters used in the fit to experimental data in (Bannister and Thomson, 2007).

resources reach certain level, then the change to a novel, lower frequency, due to a longer inter-spike interval, allows for partial restoration of the recovered resources and the next PSC is larger. Hence one can see that after a period of intense stimulation the synapse becomes sensitive to the cessation of the stimulation.

However in case of the cat layer 4 to layer 3 connections shown in sec. 3.1.3, where the fitted $\tau_{\mathrm{i}}$ (12 ms) is of the same order as $\tau_{\mathrm{r}}$ (47 ms) one can see that a transition to lower frequency attenuates the PSC in Fig 7(c). Moreover a transition to a sufficiently higher frequency amplifies the signal due to PSC summation. As a consequence there is a frequency range the transition depresses the PSC even more. In this aspect this synapse resembles a notch-filter.

In Fig. 6(b), 6(d), 7(b)-7(f), 8(b)-8(f) we present the amplitude of the second PSC relative to the amplitude of the first PSC after the frequency change for the three datasets. In those figures one can observe an interesting property: upon the decrease of frequency $f$ to a novel frequency $F$ the measure has a well marked maximum. The novel frequency $F$ at which the $A_{\mathrm{II}}$ has maximum for given $f$ increases slightly with $f$, but stays in a quite narrow frequency band. This behavior is not obvious after analyzing $A_{\mathrm{I}}$. As the frequency of stimulation changes from higher $f$ to lower $F$ one expects that after the first increased PSC the consecutive PSC would display the depressing property of the synapse, that is their amplitude would monotonically decrease or increase towards its new stationary value for the novel frequency $F$. However, the measure $A_{\mathrm{II}}(f, F)$ in all the above mentioned figures clearly shows that there is a distinct frequency band such that the reduction of stimulation frequency for $f$ to that band results not only in amplification of the first PSC but also of the consecutive one. Hence the depressing synapse is not only an 'off-synapse', sensitive to the cessation of the stimulation, but it is also specifically sensitive to the change of the stimulation frequency to a particular lower frequency, a *characteristic* frequency of the given synapse.

In case of the cat layer 4 to layer 3 connection the preferred frequency in Fig. 7(d) is much lower than the 'unpreferred' frequency in Fig. 7(e).

The average firing frequency of neurons of the suprachiasmatic nucleus is 7 Hz. In Fig. 9(a) and 6(b)

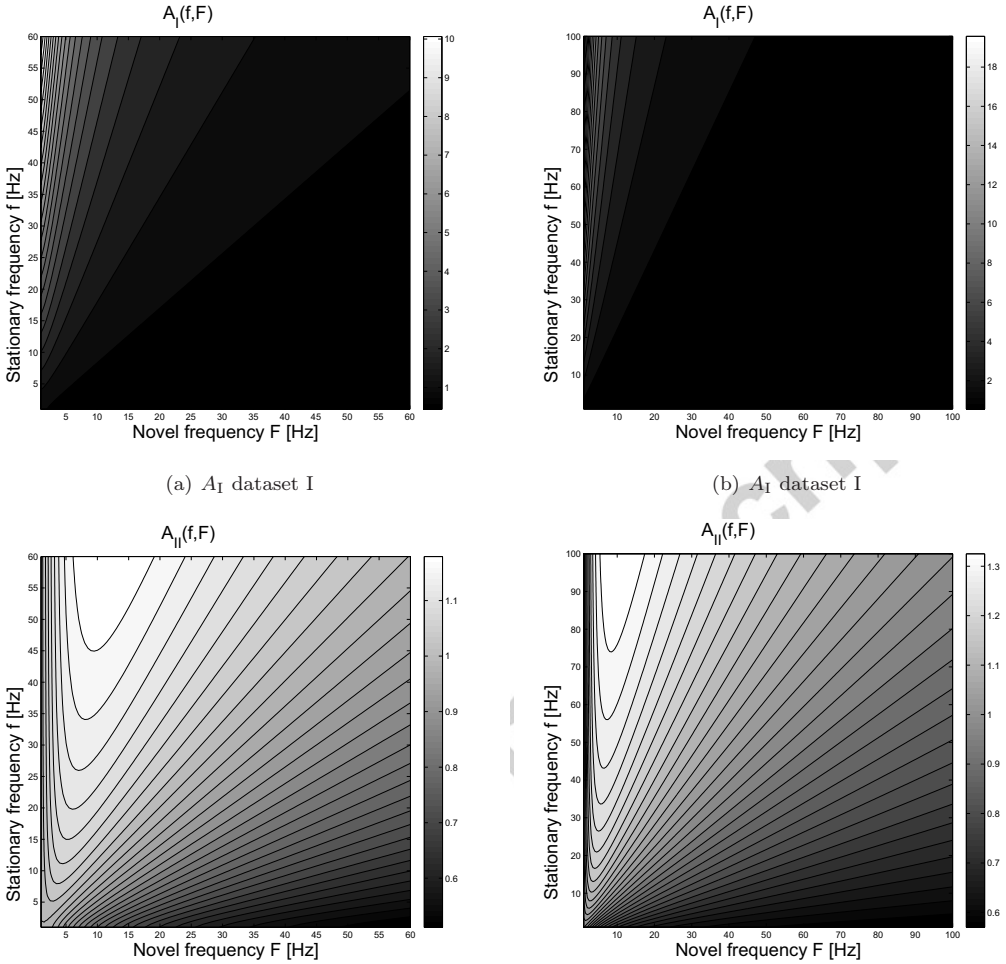


(a) $A_{\mathrm{I}}$ dataset I

(b) $A_{\mathrm{I}}$ dataset I

(c) $A_{\mathrm{II}}$ dataset I

(d) $A_{\mathrm{II}}$ dataset II

Figure 6: (a) Ratio of the first PSC after the frequency change to the PSC in the stationary mode (21) in synapses described in (Gompf and Allen, 2004) (b) Ratio of amplitudes of the second PSC to the first PSC after the change of the frequency in the stationary mode (22) in synapses from (Gompf and Allen, 2004) (c) Ratio of the first PSC after the frequency change to the PSC in the stationary mode (21) in synapses described in (Petersen, 2002) (d) Ratio of amplitudes of the second PSC to the first PSC after the change of the frequency in the stationary mode (22) in synapses from (Petersen, 2002)

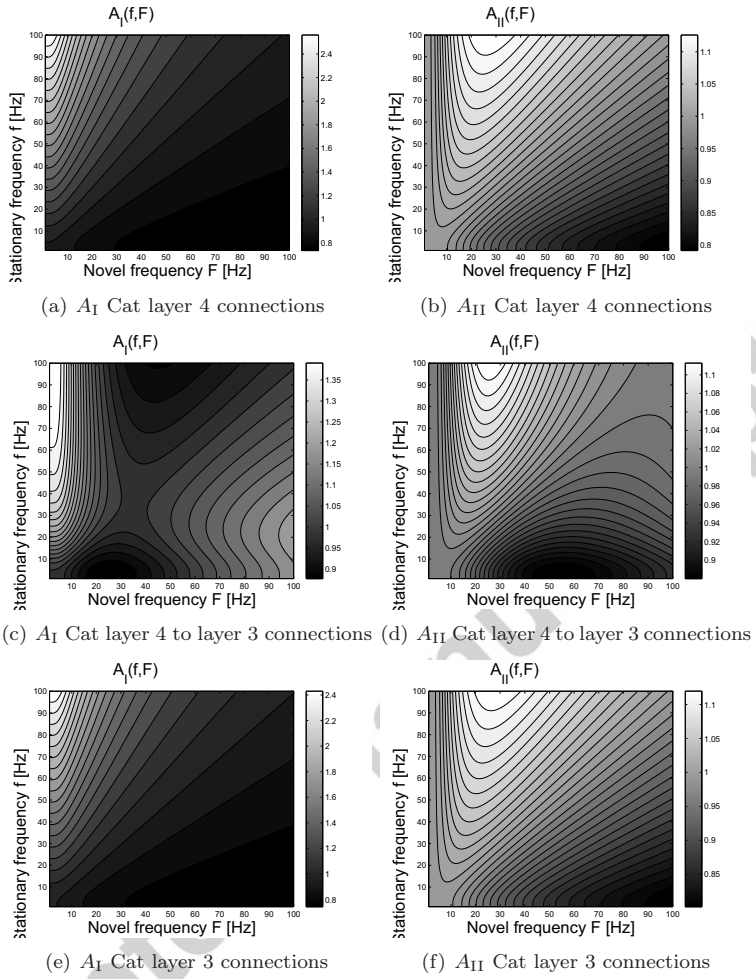


(a) $A_{\mathrm{I}}$ Cat layer 4 connections (b) $A_{\mathrm{II}}$ Cat layer 4 connections

(c) $A_{\mathrm{I}}$ Cat layer 4 to layer 3 connections (d) $A_{\mathrm{II}}$ Cat layer 4 to layer 3 connections

(e) $A_{\mathrm{I}}$ Cat layer 3 connections (f) $A_{\mathrm{II}}$ Cat layer 3 connections

Figure 7: (a) Ratio of the first PSC after the frequency change to the PSC in the stationary mode (21) in cat layer 4 connections (b) Ratio of amplitudes of the second PSC to the first PSC after the change of the frequency in the stationary mode (22)in cat layer 4 connections (c) Ratio of the first PSC after the frequency change to the PSC in the stationary mode (21) in cat layer 4 to layer 3 connections (d) Ratio of amplitudes of the second PSC to the first PSC after the change of the frequency in the stationary mode (22) in cat layer 4 to layer 3 connections (e) Ratio of the first PSC after the frequency change to the PSC in the stationary mode (21) in cat layer 3 connections (f) Ratio of amplitudes of the second PSC to the first PSC after the change of the frequency in the stationary mode (22)in cat layer 3 connections

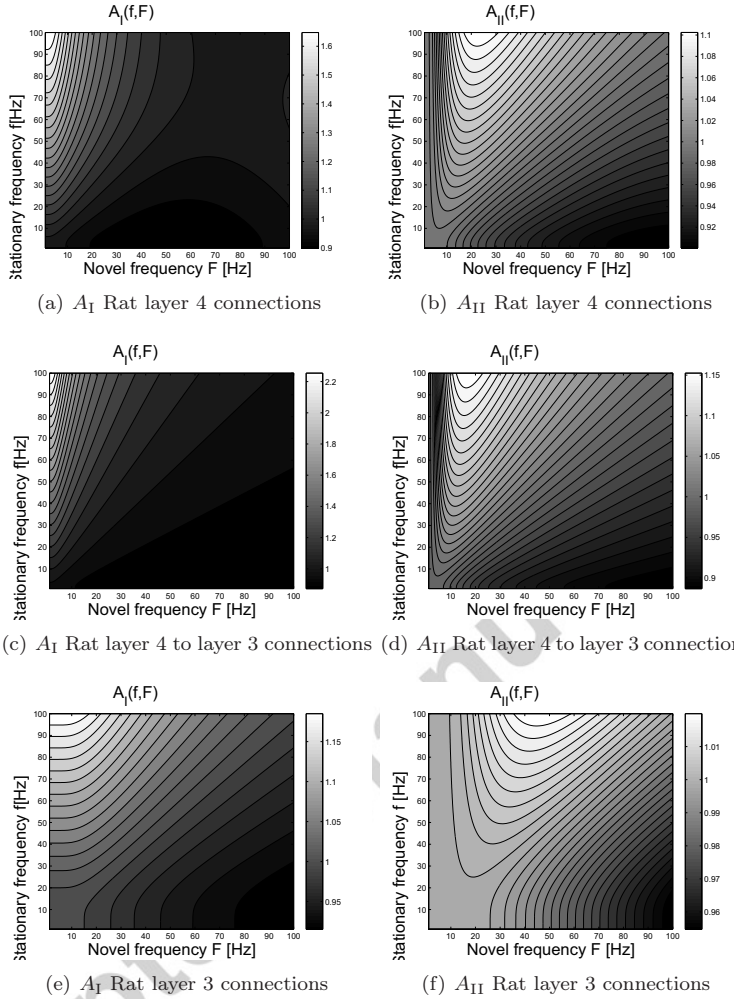


(a) $A_{\mathrm{I}}$ Rat layer 4 connections (b) $A_{\mathrm{II}}$ Rat layer 4 connections

(c) $A_{\mathrm{I}}$ Rat layer 4 to layer 3 connections (d) $A_{\mathrm{II}}$ Rat layer 4 to layer 3 connections

(e) $A_{\mathrm{I}}$ Rat layer 3 connections (f) $A_{\mathrm{II}}$ Rat layer 3 connections

Figure 8: (a) Ratio of the first PSC after the frequency change to the PSC in the stationary mode (21) in rat layer 4 connections (b) Ratio of amplitudes of the second PSC to the first PSC after the change of the frequency in the stationary mode (22)in rat layer 4 connections (c) Ratio of the first PSC after the frequency change to the PSC in the stationary mode (21) in rat layer 4 to layer 3 connections (d) Ratio of amplitudes of the second PSC to the first PSC after the change of the frequency in the stationary mode (22) in rat layer 4 to layer 3 connections (e) Ratio of the first PSC after the frequency change to the PSC in the stationary mode (21) in rat layer 3 connections (f) Ratio of amplitudes of the second PSC to the first PSC after the change of the frequency in the stationary mode (22)in rat layer 3 connections

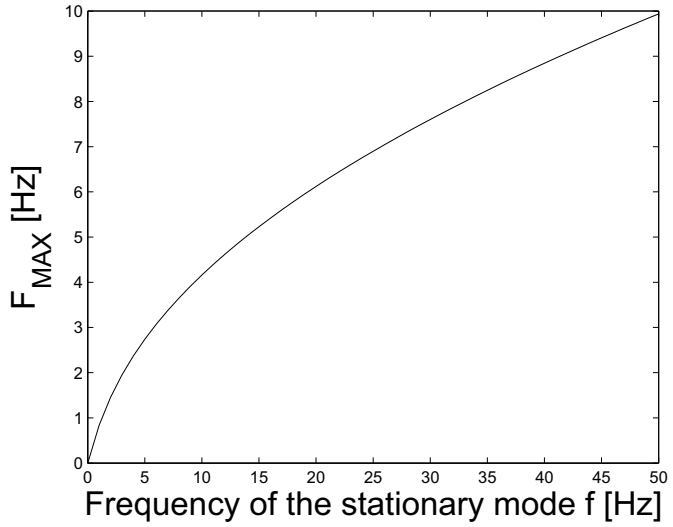


(a) Transition frequency assuring maximum $A_{\mathrm{II}}$ amplification for dataset I

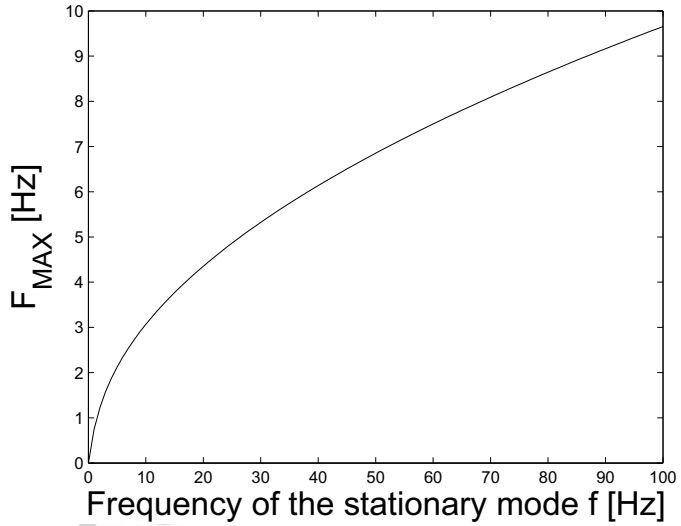


(b) Transition frequency assuring maximum $A_{\mathrm{II}}$ amplification for dataset II

Figure 9: Plots of transition frequency assuring maximum $A_{\mathrm{II}}$ amplification for datasets I and II calculated using the two-state model (26).

one can see that this frequency gives the highest amplification for the transition from frequencies higher that 20 Hz. One can also see that contrary to what one would anticipate — frequency transition to 2 Hz amplifies the PSC to a lesser extent than the frequency transition to 7 Hz. In case of the synapses of the neurons from the barrel cortex, as it can be seen in Fig. 9(b) and 6(d) it seems that frequency 10 Hz and its neighborhood is favored in transitions from higher frequencies.

In the third dataset one can see that in the case of cat connections the preferred frequency band is between 20 and 40 Hz, with the maximum close to 20 Hz. In case of the cat layer 4 layer 3 connections the frequency band is narrower, between 20 and 30 Hz. The unpreferred transition is from frequencies $f > 30$ Hz to $F > 35$ Hz.

The rat layer 4 connections the preferred frequency band is between 15 and 25 Hz with its maximum close to 25 Hz. Rat layer 3 pyramidal-pyramidal connections do not exhibit a pronounced amplification for a transition to any frequency band in the considered frequency range.

## 4. Discussion and conclusions

Short term synaptic depression is a very interesting phenomenon and one can find many attempts to model it in literature. One of the easiest and most popular is the use-dependent model (Varela et al., 1997, 1999; Markram et al., 1998; Markram and Tsodyks, 1996; Abbott et al., 1997). The synaptic resources can be found in two states — ready $R$, and used $(1 - R)$. An action potential releases only a fraction ($U_{\mathrm{SE}}$) of the releasable resources $R$ at a synaptic connection. The total amount of resources is constant.

The TM-model (1) is more complicated as it assumes, that the resources can be in three states — recovered, effective, and inactive — in order to better describe the dynamics of synaptic vesicles. Usually one assumes that as the AP arrives the $U_{\mathrm{SE}}$ fraction of recovered resources increases the effective fraction. It was shown in (Mazurkiewicz et al., 2008) that assuming a step form of the delta function in (1) it is equivalent to the receptor desensitization model proposed by Destexhe et al. (1994a,b).

The finite solutions found in (Mazurkiewicz et al., 2008) computed assuming different finite synapse stimulation durations converge to the limiting solution (8) as anticipated.

The regularization of TM model proposed by Mazurkiewicz et al. (2008) enabled finding a closed form solution of the model's equations. The analysis of dependence of those solutions on the parameters indicated that duration of synaptic stimulation has weak influence on the model properties. In this paper we presented a next step—we found the asymptotic form of the model with the stimulation time approaching 0. Indeed taking that limit results in a plausible and simple model. Formulas (12) and (16) derived from the model were used to validate the model against the experimental data. As was shown in Figs. 3 and 4 we fitted the model to the experimental data from (Gompf and Allen, 2004), (Petersen, 2002) and (Bannister and Thomson, 2007), and obtained a good fit, and the estimated parameters are in the physiologically plausible range. In case of the third dataset (sec. 3.1.3 data from (Bannister and Thomson, 2007)) one can also see that the best-fit $U_{\mathrm{SE}}$ values are roughly the same for all rat connections and for all cat connections. One can also see that all the cat recovery constants are in agreement, that also indicates that the three-step model might reflect a proper physiological mechanism underlying synaptic depression.

The closed form of formulas for popular measures of the short term synaptic depression effect, namely the *PPR* and *PPD* give us a better insight into the relation between the model parameters and the effect of depression. Specifically, we were able to demonstrate the dependence of depression on the inactivation $\tau_{\mathrm{i}}$ and recovery $\tau_{\mathrm{r}}$ time constants. For the physiological range of stimulating

frequencies (1–100 Hz) and typical orders of $\tau_{\mathrm{i}} \sim 1$ ms and $\tau_{\mathrm{r}} \sim 10^2$ ms the depth of depression strongly depends on the $\tau_{\mathrm{r}}$ constant. The derivation of *PPR* and *PPD* forms was based on calculation of the PSC related to the first and the second action potential in a series. We demonstrated that the analytical, iterative forms of the model evolution can be extended for any number of action potentials. This gives us the fast way for computing the synapse response for any action potential sequence. This approach lets us also estimate the asymptotic values of the model state variables.

The synapses in vivo are continuously exposed to incoming stimulations. It is thus interesting to investigate the reaction of the synapse to changes in the interspike intervals. For the sake of simplicity we investigated an idealized situation. The synapse was operating in the stationary mode that is, it was stimulated for a certain time (long enough to reach the asymptotic values of resources). Then at some moment, the input frequency was changed to a novel value. In order to quantify the reaction of the synapse we introduced two measures: $A_{\mathrm{I}}$—relative amplitude of the first PSC after the frequency change to the PSC before the frequency change, and $A_{\mathrm{II}}$—the relative amplitude of the second PSC after the frequency change to the first one.

We found that the $A_{\mathrm{I}}$, indicates pronounced increase of PSC in case of transition from higher to a lower frequency. The higher the ratio of the frequency of the stationary mode to the novel frequency, the bigger the increase. This dependence in monotonic. However, in case of the $A_{\mathrm{II}}$ when switching from a higher stationary frequency to a lower novel frequency, here is a novel frequency that results in a maximal value of $A_{\mathrm{II}}$. That characteristic frequency depends only slightly on the preceding stationary frequency. In this sense we can say that for a given synapse there is a preferred frequency band.

In case of the inactivation time constant of the order of the recovery time-constant the behaviour of the synapse is more complicated — exhibiting a band-pass properties and a notch filter properties.

Therefore a more complete view of functioning of the depressing synapse emerges. The synapse works as a filter of high frequency inputs since the PSC induced by a series of fast action potentials quickly diminish. The synapse can signal the cessation of high frequency input as the next AP after a longer interspike interval induces a stronger PSC. The return from high frequency stimulation to the preferred frequency band is signaled specifically.

Abbott, L., Varela, J., Sen, K., Nelson, S., 1997. Synaptic depression and cortical gain control. Science 275, 220.

Baldelli, P., Fassio, A., Valtoria, F., Benfenati, F., 2007. Lack of synapsin i reduces the readily releasable pool of synaptic vesicles at central inhibitory synapses. The Journal of Neuroscience 27, 13520.

Bannister, A. P., Thomson, A. M., 2007. Dynamic properties of excitatory synaptic connections involving layer 4 pyramidal cells in adult rat and cat neocortex. Cerebral Cortex 17 (9), 2190.

Destexhe, A., Mainen, Z. F., Sejnowski, T. J., 1994a. Synthesis of models for excitable membranes, synaptic transmission and neuromodulation using a common kinetic formalism. Journal of Computational Neuroscience 1 (3), 195.

Destexhe, A., Mainen, Z. F., Sejnowski, T. J., 1994b. Synthesis of models for excitable membranes, synaptic transmission and neuromodulation using a common kinetic formalism. Neural Computation 6, 14.

Dobrunz, L. E., Huang, E. P., Stevens, C. F., 1997. Very short-term plasticity in hippocampal synapses. Proceedings of the National Academy of Sciences of the United States of America 94, 14843.

Finnerty, G., Roberts, L., Connors, B., 1999. Sensory experience modifies the the short-term dynamics of neocortical synapses. Nature 400, 367.

Gompf, H. S., Allen, C. N., 2004. Gabaergic synapses of the suprachiasmatic nucleus exhibit a diurnal rythm of short-term synaptic plasticity. European Journal of Neuroscience 19, 2791.

Inouye, S.-I. T., Kawamura, H., 1979. Persistence of circadian rhythmicity in a mammalian hypothalamic island containing the suprachiasmatic nucleus. Proceedings of the National Academy of Sciences of the United States of America 76 (11), 5962.

Markram, H., Tsodyks, M. V., 1996. Redistributionf of synaptic efficacy between neocortical pyramid neurons. Nature 382, 807.

Markram, H., Wang, Y., Tsodyks, M., 1998. Differental signalling via the same axon of neocortical pyramidal neurons. Proceedings of the National Academy of Sciences of the United States of America 95, 5323.

Mazurkiewicz, J., Żygierewicz, J., Korzyński, M., 2008. Short term synaptic depression model - analytical solution and analysis. Journal of Theoretical Biology.

Nadel, L., Cooper, L., Culicover, P., Harnish, R. M. (Eds.), 1989. Neural Connections, Mental Computation. MIT Press, Cambridge, MA.

Petersen, C. C. H., 2002. Short-term dynamics of synaptic transmission within the excitatory neuronal network of rat layer 4 barrel cortex. Journal of Neurophysiology 87 (6), 2904.

Stevens, C. F., Wang, Y., 1995. Facilitation and depression at single central synapse. Neuron 14, 795.

Sun, H. Y., Lyons, S. A., Dobrunz, L. E., 2005. Mechanisms of target-cell specific short-term plasticity at schaffer collateral synapses onto interneurones versus pyramidal cells in juvenile rats. Journal of Physiology 568 (3), 815.

Takayasu, Y., Iino, M., Shimamoto, K., Tanaka, K., Ozawa, S., 2006. Glial glutamate transporters maintain one-to-one relationship at the climbing fiber–purkinje cell synapse by preventing glutamate spillover. The Journal of Neuroscience 26, 6563.

Thomson, A. M., 1997. Activity-dependent properties of synaptic transmission at two classes of connections made by rat neocortical pyramidal axons *in vivo*. Journal of Physiology 502 (1), 137.

Tsodyks, M. V., Markram, H., 1997. The neural code between neocortical pyramidal neurons depends on neurotransmitter release probability. Proceedings of the National Academy of Sciences of the United States of America 94 (2), 719.

Varela, J., Sen, K., Gibson, J., Fost, J., Abbott, L., Nelson, S., 1997. A quantitative description of short-term plasticity at excitatory synapses in layer 2/3 of rat primary visual cortex. Journal of Neuroscience 17, 7926.

Varela, J., Song, S., Turrigiano, G., Nelson, S., 1999. Differntial depression at excitatory and inhibitory synapses in visual cortex. Journal of Neuroscience 19, 4293.

Wall, M. J., 2005. Short-term synaptic plasticity during development of rat mossy fibre to granule cell synapse. European Journal of Neuroscience 21, 2149.

West, D. C., Mercer, A., Kirchhecker, S., Morris, O. T., Thomson, A. M., 2006. Layer 6 cortico-thalamic pyramidal cells preferentially innervate interneurons and generate facilitating epsps. Cerebral Cortex 16 (2), 200.